

# The EUV lithography resist screening activities in H2-2022

Aysegul Develioglul<sup>a</sup>, Tim P. Allenet<sup>a</sup>, Michaela Vockenhuber<sup>a</sup>, Lidia van Lent-Protasova<sup>b</sup>,  
Iacopo Mochi<sup>a</sup>, Yasin Ekinici<sup>a</sup>, Dimitrios Kazazis<sup>a</sup>

<sup>a</sup> Paul Scherrer Institut, 5232, Villigen-PSI, Switzerland

<sup>b</sup> ASML, De Run 6501, 5504 DR Veldhoven, The Netherlands

## ABSTRACT

EUV resist materials are crucial for enabling next-generation lithographic technologies that aim to achieve high-volume manufacturing (HVM) at sub-5 nm nodes. In this study, we report an extensive performance characterization of EUV photoresists for future high-NA EUV lithography. We investigated the performance of various resists using the EUV interference lithography tool at the Swiss Light Source (SLS) within the framework of a collaboration between the Paul Scherrer Institute and ASML. This paper presents the major outcomes of the work conducted in the second half of 2022. Important performance characteristics taken into account in this study are resolution or half-pitch (HP), dose-to-size (DtS) and line-width roughness (LWR). To evaluate the overall performance of the resists, we used the Z-factor. We investigated both chemically amplified resists (CAR) and non-CAR materials. CARs from two vendors achieved a resolution down to 11 nm half-pitch, while multi-trigger resists (MTR) reached a resolution of 13 nm. In comparison, MTRs demonstrated better Z-factor values owing to their high sensitivity. In addition, we investigated the effect of underlayers on the performance of metal organic resists (MOR). We, finally, discuss the overall progress in resist performance over recent years. We observed a steady improvement across several resist platforms, which is encouraging for global EUV resist development towards high-NA EUVL.

**Keywords:** EUVL, Photoresist, High-NA, Interference Lithography

## 1. INTRODUCTION

In order to keep up with Moore's Law<sup>1</sup>, the semiconductor industry has adopted EUV lithography for high-volume manufacturing (HVM) of leading-edge computer chips. To continue the downscaling for future technology nodes, high-NA lithography will be indispensable. Yet, finding a suitable photoresist for high-NA patterning remains a major challenge. To address this by supporting the global resist development activities of academic and industrial researchers, PSI and ASML have been collaborating for several years<sup>2-4</sup> on a joint research program aimed at providing a performance screening platform to help resist developers overcome this challenge.

The XIL-II beamline at the Swiss Light Source (SLS), PSI, is dedicated to EUV lithography and metrology and features a dedicated cleanroom with an exposure tool based on EUV interference lithography (IL) and resist processing capabilities. After exposure and development, the resists are inspected by scanning electron microscopy (SEM) using an ultra-high resolution tool, following a standard inspection protocol. The SEM images are subsequently analyzed using a specifically designed software<sup>5</sup> to extract the performance metrics: critical dimension (CD), dose-to-size (DtS), and line-width roughness (LWR). We also take the Z-factor<sup>6</sup> into account to provide a shorthand assessment of the overall resist performance.

In this study, we report on the resist performance results obtained in the second half of 2022 for patterning of line/space (L/S) patterns for future technology nodes. We investigated more than 100 resist materials, from six different vendors for existing NXE and future high-NA scanners. We begin by describing the exposure tool and our methodology used for the resist evaluation, and then showcase the best-performing resists for half-pitches (HPs) ranging from 14 down to 10 nm. We also demonstrate the evolution of the resist materials over the past three years.

## 1.1 EUV interference lithography

IL is a patterning method in which two or more mutually coherent beams interfere on the wafer plane and create a periodic aerial image. The beam used in our exposure tool has high spatial coherence and a bandwidth of 4% and a central wavelength of 13.5 nm.<sup>7</sup> The mutually coherent beams in this case are obtained by illuminating a pair of transmission diffraction gratings on a thin silicon nitride membrane. The fabrication process of such gratings has been reported elsewhere.<sup>8</sup> The two diffracted beams are designed to interfere on the resist surface and create periodic L/S patterns, as shown in Figure 1. The intensity distribution of the aerial image is determined by the constructive and destructive interference of the two diffracted beams, given by

$$I(x) = \cos^2\left(\pi \frac{x}{p}\right)$$

where  $p$  is the pitch of lines and spaces.<sup>9</sup> Furthermore, the pitch of the aerial image is half of the pitch of the diffraction gratings on the mask.

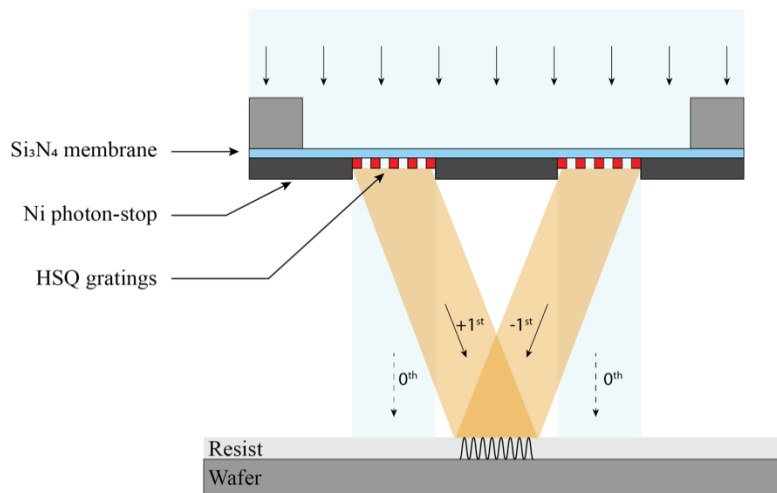


Figure 1. Schematic of the EUV-IL method. The two diffracted beams interfere and create a periodic aerial image with high contrast, which is recorded into the photoresist.

This method of patterning has several advantages. High resolution, owing to frequency multiplication as well as high and focus-independent contrast are of paramount importance.<sup>10-11</sup> The theoretical resolution limit of this method is 3.5 nm HP and the record of achieved resolution is 6 nm HP limited by tool or resist performance.<sup>12</sup> The exposure tool provides high-resolution patterning before high-NA EUV scanners become available, it has no limitations in terms of the outgassing of resist materials, and can work with small amounts of resists. Therefore, it helps early development of EUV resists with quick turnaround and it is an important asset for both academia and industry for the timely development of EUV resists.

## 1.2 Experimental procedure

The resist screening procedure starts with coating and baking followed by an exposure of the resists with varying dose. After exposing, post-exposure baking, and developing, the wafers are inspected using a Hitachi Regulus 8230 ultra-high resolution SEM. The SEM parameters have been set along the same lines as the roughness protocol of IMEC as much as it is possible, given the fact that we use an analytical SEM and not a CD-SEM. The key parameters of the acquisition are shown in Table 1.

Table 1: SEM parameters used for resist screening

<b>Specimen current (measured)</b>	8 pA
<b>Landing voltage</b>	0.5 kV
<b>Pixel size</b>	0.83 nm
<b>Acquisition mode</b>	Charge suppression scan

We then use an open-source software developed in-house at PSI to analyze the resist images (SMILE). For each image, we extract the average CD, the local CD uniformity and the unbiased LWR ( $LWR_{\text{unb}}$ ) (Figure 2).

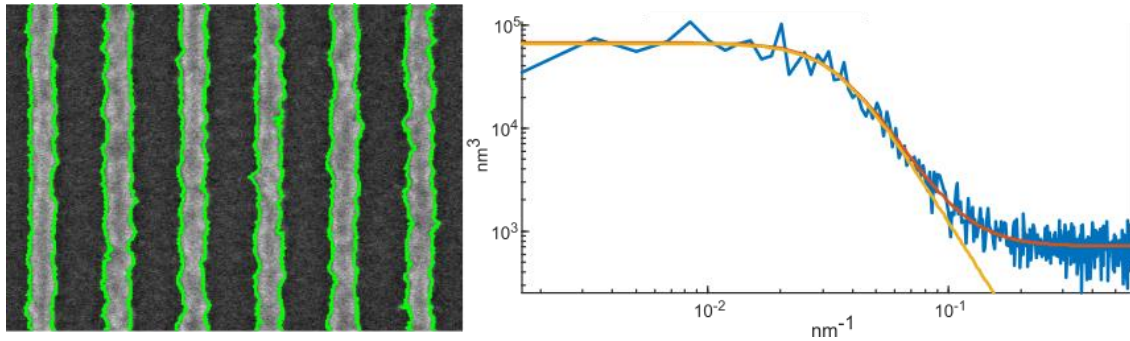


Figure 2. An example of the L/S edge detection provided by SMILE to extract the CD and the corresponding PSD curve fitting to obtain  $LWR_{\text{unb}}$ .

The acquired CD and  $LWR_{\text{unb}}$  data are plotted as a function of the exposure dose and the data is fitted using polynomial fit to determine the Dts and corresponding  $LWR_{\text{unb}}$ . We note that the photon dose at the wafer level has been cross-calibrated with other tools.<sup>4</sup>

### 1.3 Program goals

The main target of the program is to characterize and optimize resist materials for the actual 0.33 NA systems with sub-13 nm resolution as well as to support the industry and boost the resist development towards high NA with resolutions down to 8 nm. Table 2 shows the general guidelines targeted in the resist screening program.

Table 2: General guidelines targeted in the resist screening program.

<b>Features</b>	<b>16 nm – 8 nm LS</b>
<b>Resist type</b>	CAR, non-CAR
<b>Resist thickness</b>	20 – 30 nm
<b>Throughput</b>	DTS < 60 mJ/cm <sup>2</sup>
<b>Roughness</b>	< 10%
<b>General performance</b>	Z-factor = $CD^3 \cdot LWR^2 \cdot DTS$

## 2. RESULTS

In this section, we present the results obtained in the second half of 2022, from 14 nm HP and towards higher resolutions. We present the best results considered for 14 nm HP from three positive-tone CAR and one negative-tone MTR. In addition, we have also investigated the effect of different underlayers on a particular metal-organic resist (MOR).

Figure 3 shows the highlights of 14 nm HP from three positive tone CARs and one negative tone MTR. All the resists have well-defined, well-resolved, and defect-free lines.

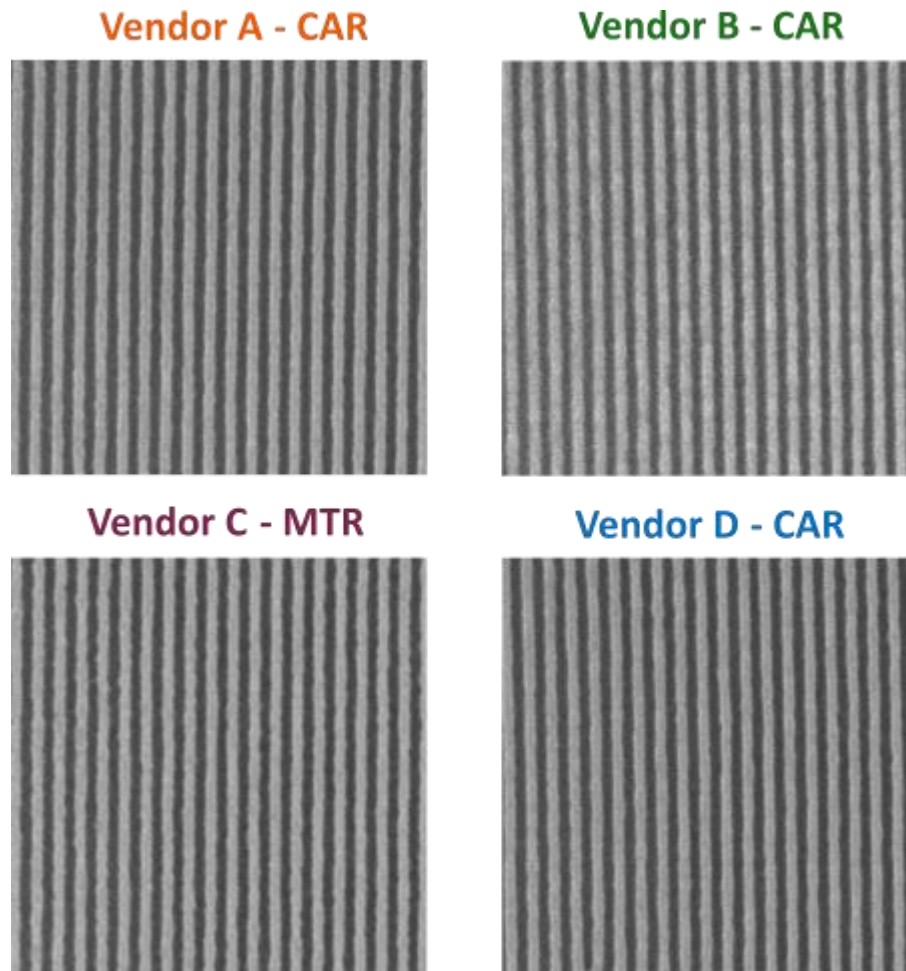


Figure 3. SEM images of best performing resists for HP 14 nm.

Table 3 shows the performance metrics of the resists in Figure 3 with the general guidelines for HP 14 nm. All resists meet the DtS target. However, Vendor C - MTR has significantly lower DtS and is the only resist that meets the Z-factor criterion. All vendors' resists show  $LWR_{unb}$  above the program target of 1.4 nm.

Table 3. Performance metrics of 14 nm highlights.

HP 14 nm	Vendor A - CAR	Vendor B - CAR	Vendor C - MTR	Vendor D - CAR	General guideline
Dose-to-size (mJ/cm <sup>2</sup> )	53.85	38.9	19.40	36.95	<60
Unbiased LWR (nm)	2.51	2.63	2.72	2.40	<1.4
Z-factor (x10 <sup>-8</sup> ) (mJ·nm <sup>3</sup> )	0.96	0.73	0.40	0.60	<0.46

Figure 4 shows the highlights for 13 nm HP. The SEM images are obtained from three positive tone CARs and one negative tone MTR. Vendor C - MTR shows a few defects between the lines but the CARs have well defined lines.

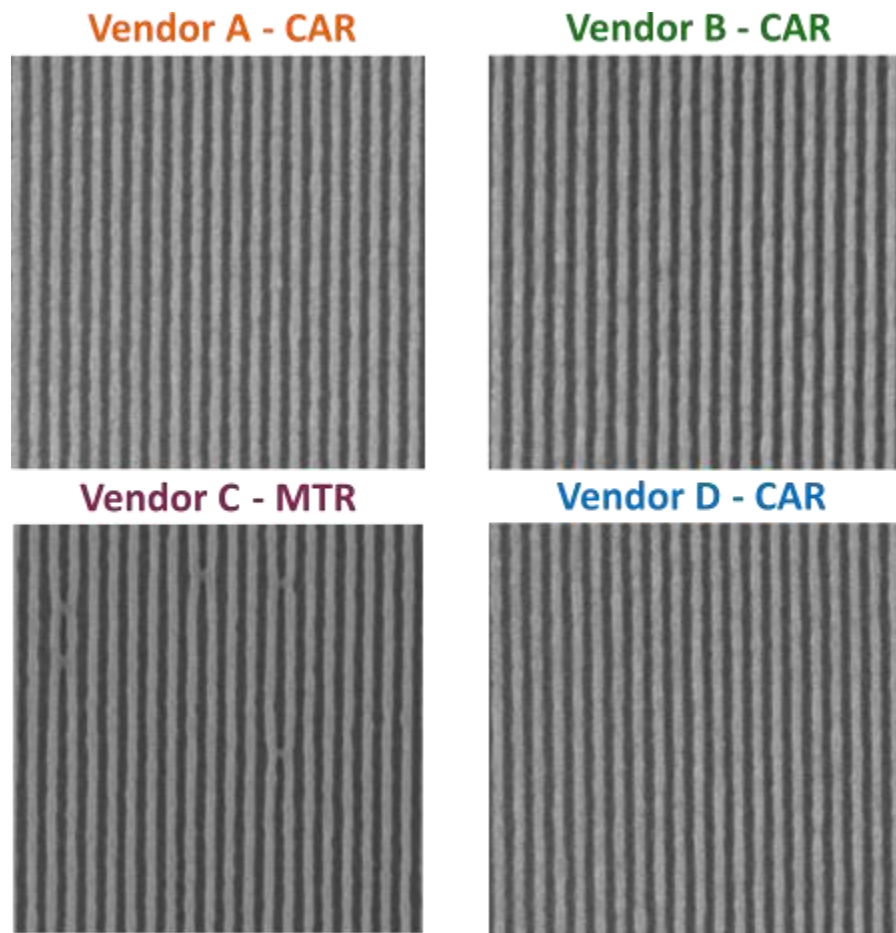


Figure 4. SEM images of the best performing resists for HP 13 nm.

Table 4 shows the performance metrics of the best resists from Figure 4 with the general guidelines for HP 13 nm. Again, all the resists meet the DtS criterion and Vendor C - MTR has the lowest value. The corresponding  $LWR_{unb}$  is above target for all the resists. Vendor C - MTR shows a Z-factor at the target owing to its high sensitivity.

Table 4. Performance metrics of 13 nm highlights.

HP 13 nm	Vendor A - CAR	Vendor B - CAR	Vendor C - MTR	Vendor D - CAR	General guidelines
Dose-to-size (mJ/cm <sup>2</sup> )	51.25	41.2	24.3	26.38	<60
Unbiased LWR (nm)	2.84	2.58	2.5	2.97	<1.3
Z-factor (x10 <sup>-8</sup> ) (mJ·nm <sup>3</sup> )	0.85	0.61	0.33	0.47	<0.32

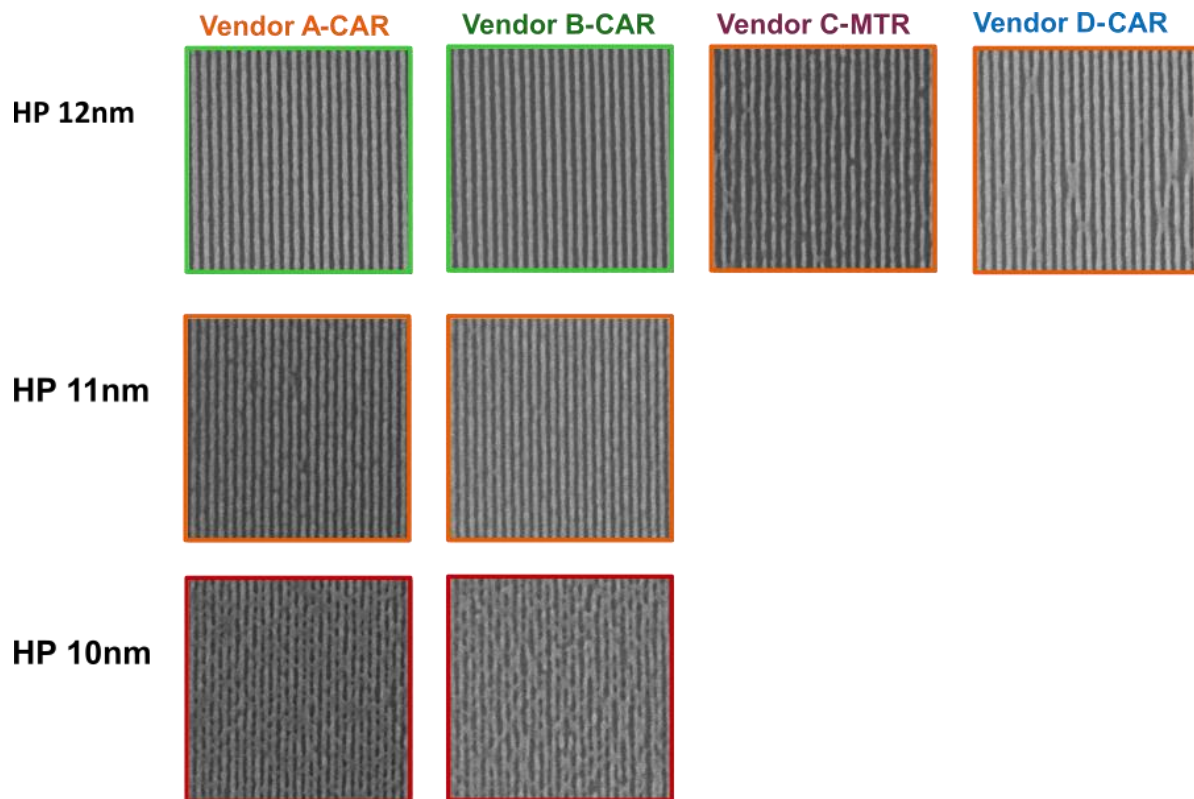


Figure 5. SEM images of the best performing resists at HP range of 12 nm to 10 nm.

Figure 5 shows the SEM images of the best performing resists at higher resolutions (smaller pitches). Vendor A - CAR and Vendor B - CAR has a resolution limit of HP 11 nm while Vendor C - MTR and Vendor D - CAR have a resolution limit of 13 nm due to broken lines and collapsed patterns. Higher resolutions require material and process optimization. However, we should emphasize that MTR and Vendor D - CAR have never been tested for higher resolutions than 12 nm HP.

Figure 6 shows the unbiased LWR vs. dose at 14 nm HP and 13 nm HP of the best performing resists of 5 vendors. The dashed line is the performance of general guidelines for CD 14 nm and CD 13 nm with constant Z-factor of 0.46 and 0.32 respectively. Filled dots show the 1:1 ratio of lines and spaces for each resist. For HP 14 nm, the MTR and one of the CARs and for HP 13 nm, only the MTR is within the iso-Z-factor line. Since the general guideline for DtS is less than 60 mJ/cm<sup>2</sup>, program objective is to reach the orange area under the dashed line.

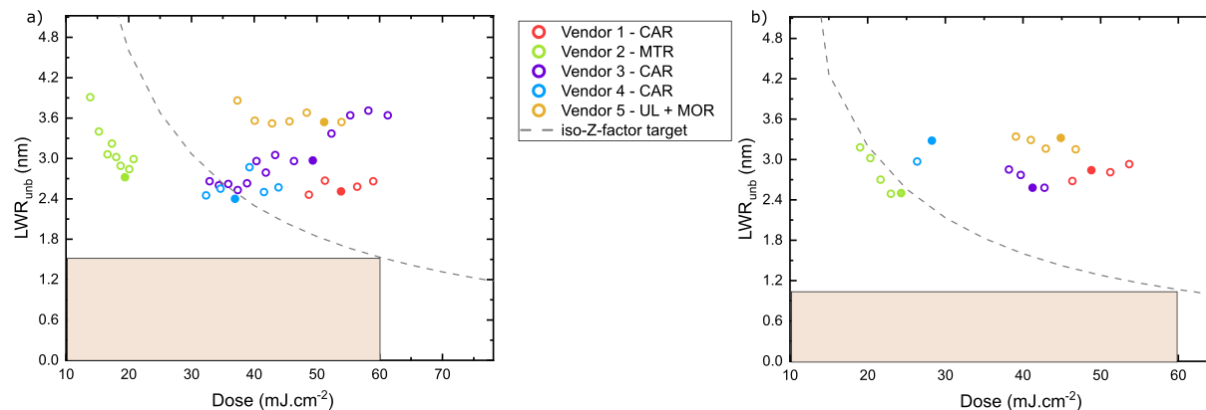


Figure 6.  $LWR_{unb}$  as a function of DtS for resist screened for a) HP 14 nm b) HP 13 nm. The dashed line is the performance of general guidelines for HP 14 nm and HP 13 nm. Filled dots show the 1:1 ratio of lines and spaces for each resists. The program objective is to reach the orange area under the dashed line.

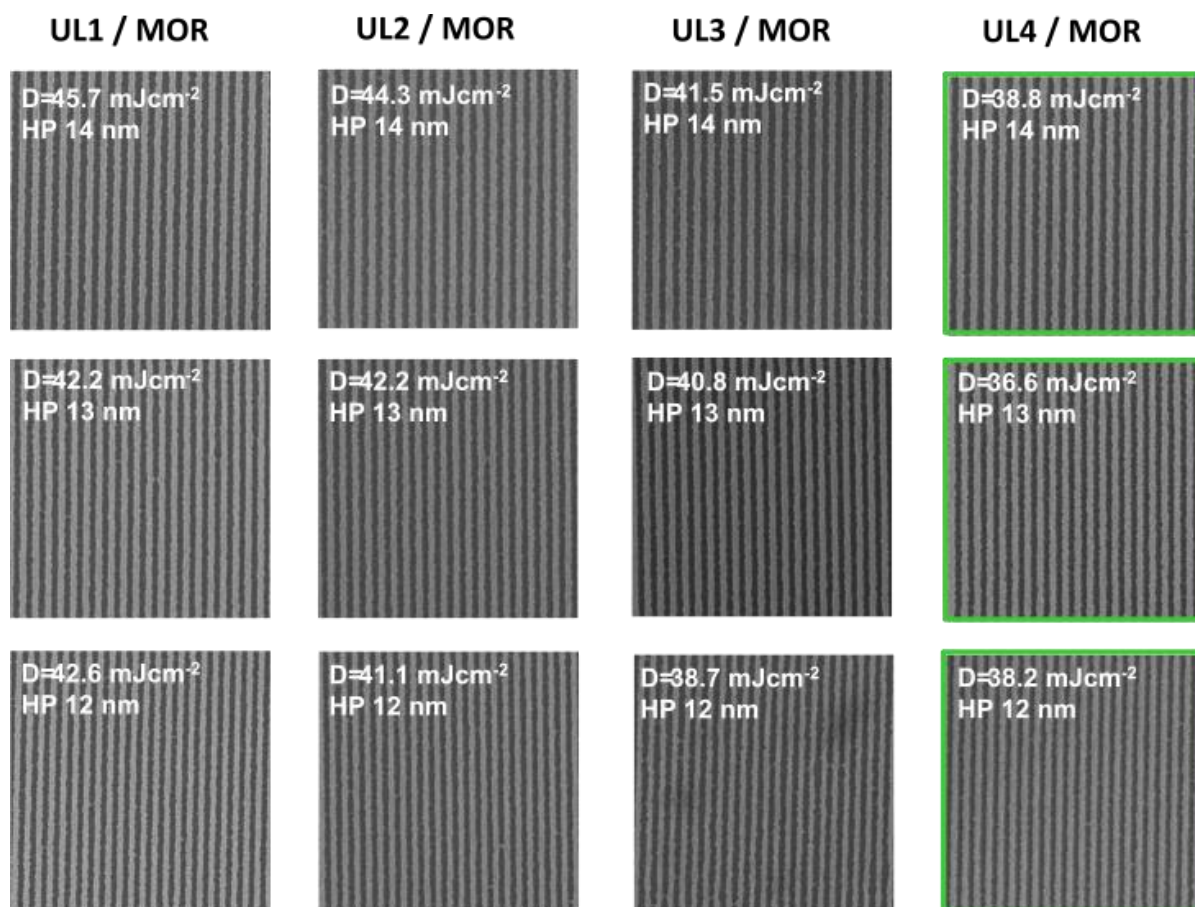


Figure 7. The performance of the same MOR with different UL for HP 14, 13, and 12 nm.

Figure 7 shows the performance of the same MOR with different underlayers (UL) for HP 14, 13, and 12 nm. DtS decreases from 45.7 mJ/cm<sup>2</sup> (UL1) to 38.8 mJ/cm<sup>2</sup> (UL4) for HP 14 nm, from 42.2 mJ/cm<sup>2</sup> (UL1) to 36.6 mJ/cm<sup>2</sup> (UL4) for HP 13 nm and from 42.6 mJ/cm<sup>2</sup> (UL1) to 38.2 mJ/cm<sup>2</sup> (UL4) for HP 12 nm. This shows that ULs can have a significant effect on the resist performance not only to promote adhesion and prevent pattern collapse but also to reduce the DtS. It is important to note that unavoidable delay between exposure and bake/development affects the quality of the lines for MOR.

Figure 8 shows the evolution of the Z-factor of the best performing CAR, MTR and MOR resists over the past 3 years<sup>4,13</sup> and SEM images of the best performing resists in terms of Z-factor. The results show a clear improvement in resist performance in all three types of resists. The clear trend of improved Z-factors over time denotes that the program targets in terms of resolution, sensitivity, and roughness are realistic and achievable in the near future.

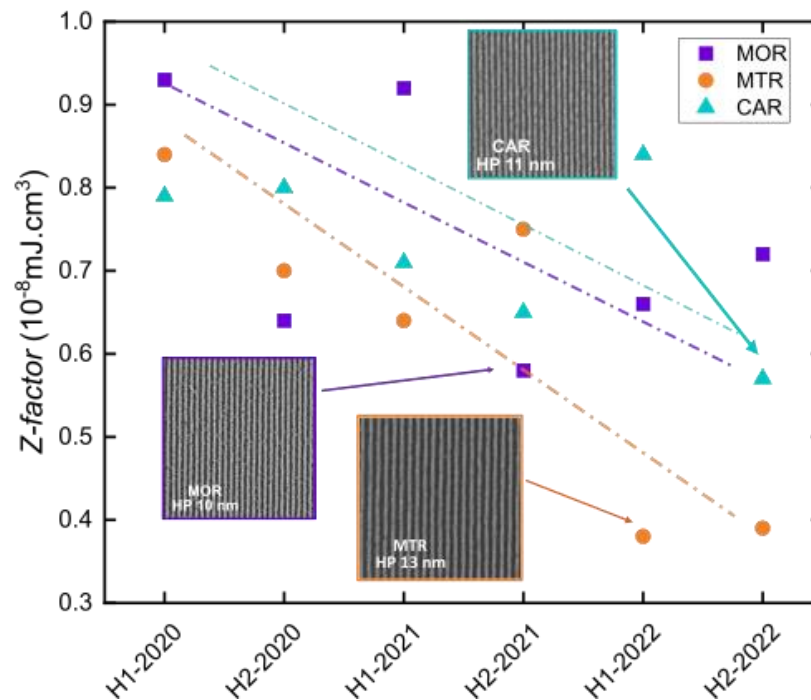


Figure 8. Z-factor evaluation of performing CAR, MTR and MOR over the past 3 years and SEM images of best performing resists in terms of Z-factor.

### 3. CONCLUSION

In this paper, we presented an update on the resist screening program carried out at PSI in collaboration with ASML. In the second half of 2022, we characterized more than 100 photoresists from six different vendors. We presented results of 14 nm resolution and beyond for three CARs and one MTR, with resolutions of 14 to 10 nm. We also investigated the effect of different ULs on a particular MOR. CARs provided from two vendors have a resolution down to HP 11 nm, while MTR has a resolution limit at HP 13 nm. However, the MTR shows better performance in terms of DtS and Z-factor. We also demonstrated that the UL plays a significant role during the exposure and development, and has a noticeable effect on the performance of MORs. The general progress in Z-factor over the last three years shows that the overall performance of all three types of resists has been improving. From the general trends, we expect that single-digit nm resolutions will be reached in the near future through further process and material optimization. We believe that viable material solutions will be available in time for high-NA EUVL tools.

PSI will continue its efforts to achieve ultimate resolution and serve the community in resist development for high NA and towards hyper-NA EUVL.

#### 4. REFERENCES

1. Tasdemir Z, Wang X, Mochi I, van Lent-Protasova L, Meeuwissen M, Custers R, Rispens G, Hoefnagels R, Ekinici Y. "Evaluation of EUV resists for 5nm technology node and beyond." International conference on extreme ultraviolet lithography SPIE, 10809, 85-94, 2018.
2. Wang X, Tasdemir Z, Mochi I, Vockenhuber M, van Lent-Protasova L, Meeuwissen M, Custers R, Rispens G, Hoefnagels R, Ekinici Y. "Progress in EUV resists towards high-NA EUV lithography." Extreme Ultraviolet (EUV) Lithography X SPIE, 10957, 19-27, 2019.
3. Van Schoot J, van Setten E, Troost K, Lok S, Stoeldraijer J, Peeters R, Benschop J, Zimmerman J, Graeupner P, Wischmeier L, Kuerz P. "High-NA EUV lithography exposure tool: program progress." Extreme Ultraviolet (EUV) Lithography XI SPIE, 11323, 15-24, 2020.
4. Allenet T, Vockenhuber M, Yeh CK, Santaclara JG, van Lent-Protasova L, Ekinici Y, Kazazis D. "EUV resist screening update: progress towards high-NA lithography." Advances in Patterning Materials and Processes XXXIX SPIE, 12055, 111-120, 2022.
5. Mochi I, Vockenhuber M, Allenet T, Ekinici Y. "Contacts and lines SEM image metrology with SMILE". Photomask Technology SPIE, 11855, 2021
6. Wallow T, Higgins C, Brainard R, Petrillo K, Montgomery W, Koay CS, Denbeaux G, Wood O, Wei Y. "Evaluation of EUV resist materials for use at the 32 nm half-pitch node." Emerging Lithographic Technologies XII. SPIE, 6921, 428-438, 2008.
7. Mojarad N, Gobrecht J, Ekinici Y. "Interference lithography at EUV and soft X-ray wavelengths: Principles, methods, and applications," Microelectronic Engineering.,143, 55-63, 2015.
8. Wang X, Kazazis D, Tseng LT, Robinson AP, Ekinici Y. "High-efficiency diffraction gratings for EUV and soft x-rays using spin-on-carbon underlayers." Nanotechnology. 33(6), 065301, 2021.
9. Fallica R, Kirchner R, Ekinici Y, Mailly D. "Comparative study of resists and lithographic tools using the Lumped Parameter Model." Journal of Vacuum Science & Technology B, Nanotechnology and Microelectronics: Materials, Processing, Measurement, and Phenomena., 34(6), 06K702, 2016,.
10. Langner A, Solak HH, Gronheid R, van Setten E, Auzelyte V, Ekinici Y, van Ingen Schenau K, Feenstra K., "Measuring resist-induced contrast loss using EUV interference lithography." Extreme Ultraviolet (EUV) Lithography SPIE, 7636, 878-888, 2010.
11. Sanchez, M.I., Hinsberg, W.D., Houle, F.A., Hoffnagle, J.A., Ito, H. and Nguyen, C.V., "Aerial image contrast using interferometric lithography: effect on line-edge roughness." Advances in Resist Technology and Processing XVI SPIE, 3678, 160-171. 1999.
12. Fan D, Ekinici Y. "Photolithography reaches 6 nm half-pitch using EUV light." Extreme Ultraviolet (EUV) Lithography VII). SPIE, 9776, 541-551, 2016.
13. Allenet T, Vockenhuber M, Yeh CK, Kazazis D, Santaclara JG, van Lent-Protasova L, Ekinici Y. "Progress in EUV resist screening by interference lithography for high-NA lithography." International Conference on Extreme Ultraviolet Lithography Vol. SPIE, 1185481-90, 2021.